Beam diagnostics

U. Raich
CERN, Geneva, Switzerland

Abstract
The instrumentation measuring beam parameters constitutes an important part of any particle accelerator. These lectures aim at giving an overview of detection and measurement techniques without going too much into details of implementation. Instruments for linear accelerators, transfer lines, and small synchrotrons are described with an emphasis on opportunities and problems specific to low-energy particle beams.

1 Introduction

An accelerator can never be better than the instruments which measure its performance. Measurement instruments play a vital role in the operation of an accelerator. They are particularly important when new machines are commissioned (a moment when new instruments are also tried for the first time) or at start-up after a long shutdown. However, also during routine machine operation it is the beam measurements that tell the operator if the machine is performing correctly or not and it is the instruments that will help him to find potential faults in accelerator components.

Beam diagnostics covers a large field of activity: some knowledge of machine physics is needed in order to understand the machine parameters to be measured and the physical effects that govern their behaviour. The physics of beam interaction with the measurement sensors must be understood in order to build the sensor itself. Highly sensitive analog electronics are needed in order to amplify usually very small signals which in addition are often very fast. Digitization and digital treatment of the signals must be performed and finally a result in the form of a complex beam parameter value, like the tune, the transverse — or longitudinal emittance, the beam orbit etc. must be extracted and displayed, requiring experience in software technologies.

Most sensors are based on one of the following physical processes:

- Interaction with electric or magnetic fields of the beam particles:

  coupling to the magnetic or electric field,

  synchrotron radiation,

  transition radiation.

- Coulomb interaction between the incident beam particle and electrons in the atomic shell of intercepting matter.
- Atomic excitation with consecutive light emission.

Table 1 lists some of the instruments used in beam diagnostics, the physical effect made use of, and the beam parameter measured.

Table 1: Instruments, measured quantities and physical effects used

Instrument	Physical effect	Measured quantity	Effect on the beam
Faraday cup	Charge collection	Intensity	Destructive
Current transformer	Magnetic field	Intensity	Non-destructive
Wall current monitor	Image current	Intensity, longitudinal density distribution	Non-destructive
Pick-up, beam-position monitor (BPM)	Electric/magnetic field	Position, trajectory, orbit	Non-destructive
Secondary emission monitor	Secondary electron emission	Transverse profile, intensity, emittance	Disturbing, at low energy: destructive
Wire scanner	Secondary emission, creation of secondary particles	Transverse profile, emittance	Slightly disturbing
Scintillator screen	Atomic excitation with light emission	Transverse profile, position	Destructive
Residual gas monitor	Ionization	Transverse profile	Non-destructive

A typical instrument consists of

- the sensor (see Table 1)
- its front-end electronics, usually a pre-amplifier and shaper installed in the machine tunnel
- cabling between the tunnel and the equipment room
- signal treatment electronics and analog-to-digital conversion in the front-end computer crate this may also include some digital input/output e.g., for status information or digital control (end switches, electronics on/off, vacuum status, amplifier gain control, etc.)
- front-end software to read out the digital data and perform digital signal treatment
- front-end computer crates all connected through a local area network which has links to the main control room
- application software running on console computers in the main control room

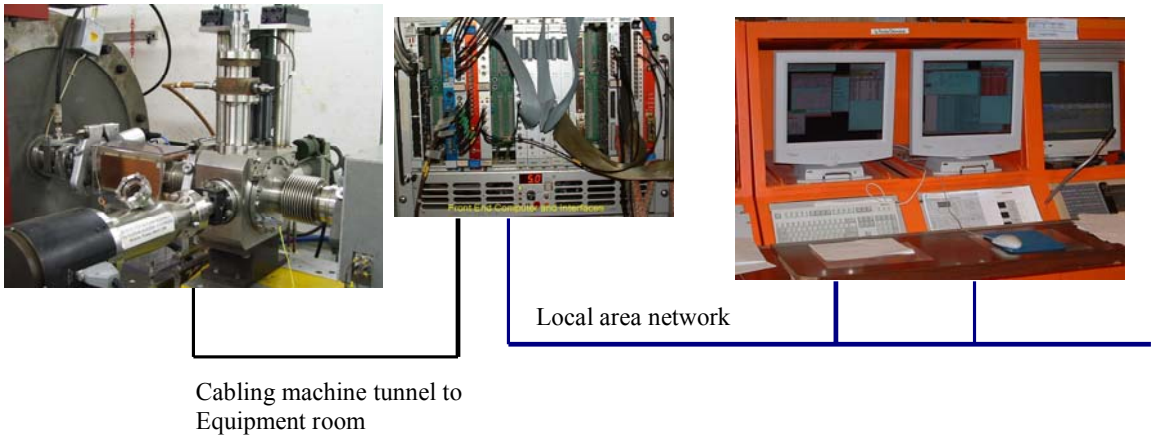

Fig. 1: A typical instrument: the sensor + front-end electronics (pre-amplifier etc.) in the tunnel (left); the front-end computer with analog-to-digital conversion (middle); the operator console with application programs (right)

2 Intensity measurements

2.1 Faraday cups

At very low energies and low intensities the Faraday cup is an often used device for intensity measurements. It acts as a beam stopper and is therefore fully destructive. An insulated metallic cup (Fig. 2 [2]) is connected to either an integrating amplifier measuring the number of incoming charges or a current-sensitive amplifier, in which case the beam current is measured. A typical set-up is shown in Fig. 3.

Very low intensities down to a few picoampere can be measured even for a DC beam with low noise current to voltage amplifiers.

Fig. 2: Photo of the Faraday cup

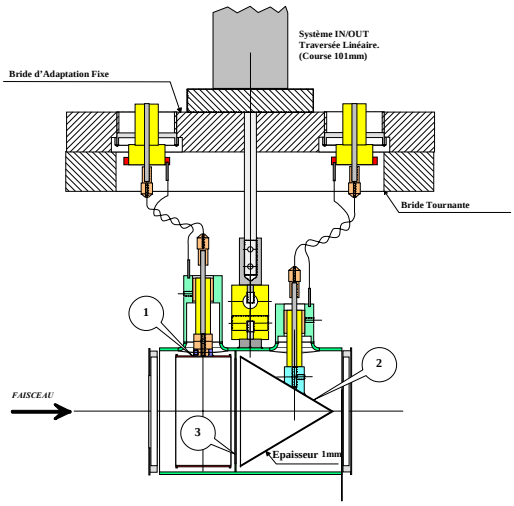

Fig. 3: A simple Faraday cup for low-intensity and low-energy beams

When a particle hits the cup's electrode surface, secondary electrons are emitted. Typical yields for incident protons of 50 keV, taking into account the cup's opening angle of 60º, are 6–7 electrons per incoming proton. The energy of these secondary electrons is very low (below 10 eV) and their flux is proportional to cos θ, where θ is the angle of the emitted electron with respect to the electrode surface. Because of their low energy, the electrons can be re-captured into the cup by applying HV to a repeller electrode (Fig. 3 [1]). A simulation of the electrostatic field within the cup when applying a –100 V repelling voltage is shown in Fig. 4, the effect on the measured current when increasing the voltage from 0 up to –100 V is displayed in Fig. 5.

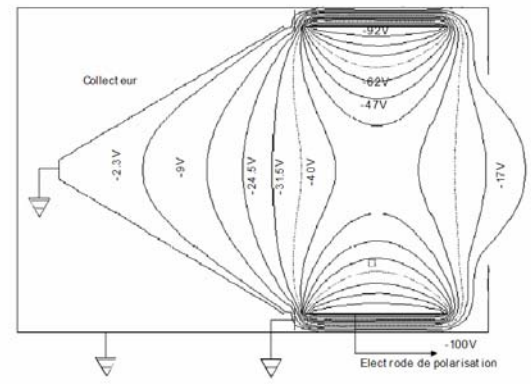

Fig. 4: Electrical field simulation in the Faraday cup with repeller voltage on

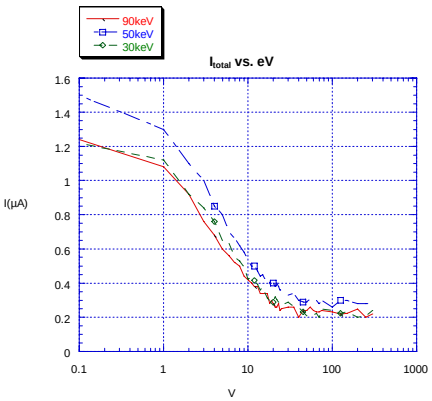

Fig. 5: Electrode current versus repeller voltage

The Faraday cup described above has a stainless steel electrode of 1 mm thickness. Protons with energy higher than 24 MeV will traverse the electrode and their charge will therefore not be captured, leading to wrong measurement results.

Increasing the beam energy and/or intensity will increase the thermal load that must be absorbed by the cup. The choice of material (high thermal conductivity) will become important and a means of cooling, e.g. water cooling, may need to be introduced.

A typical application for Faraday cups is the measurement of charge-state distributions coming form a heavy ion source. The source produces a spectrum of some 20 different ionization states from which a single one will be selected for further acceleration. The measurement uses a spectrometer magnet deflecting each of the ions with different charge state in a different way, and a slit selecting a fine slice in the spectrum. The spectrometer magnet is ramped and the current passing though the slit is recorded with a Faraday cup. Figure 6 shows a typical result for lead ions. (The negative values probably come from the beam, striking the repeller electrode which produces secondary electrons seen by the Faraday cup.)

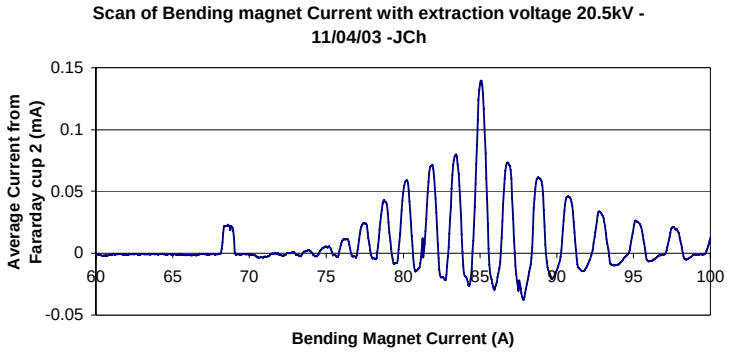

Fig. 6: Charge state spectrum from a lead-ion source measured with a Faraday cup

2.2 Current Transformers

As we know from school physics, moving charges create a magnetic field which is proportional to the current. Since a particle beam is nothing other than a collection of moving charges, it forms a current which can be described by

$$I_{\text{beam}} = \frac{qeN}{t} = \frac{qeN\beta c}{l}$$

where q is the charge state, N the number of particles, l unit of length and $\beta = v/c$ the particle speed.

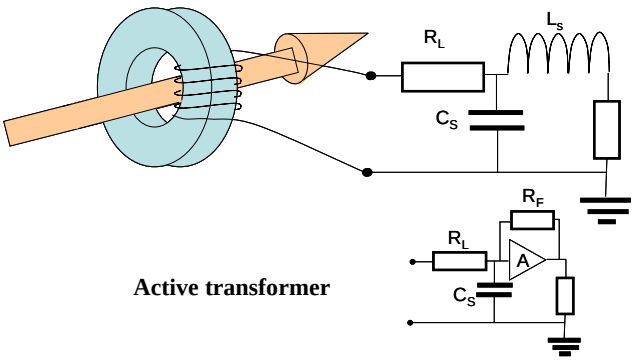

Fig. 7: Principle of a DC current transformer

The magnetic field associated with this beam can be captured using a transformer which will deliver a voltage

$$U = L\frac{\mathrm{d}I_{\mathrm{beam}}}{\mathrm{d}t}$$

in the ideal case and with infinite output impedance [see Fig. 8(a)]. If, however, we load the transformer with a finite resistance and we take into account secondary inductance and capacitance, then we get a pulse shape of the form:

$$u(t) = I_{\mathrm{beam}}(t)\frac{R}{N}e^{-\frac{t}{\tau_{\mathrm{droop}}}}.$$

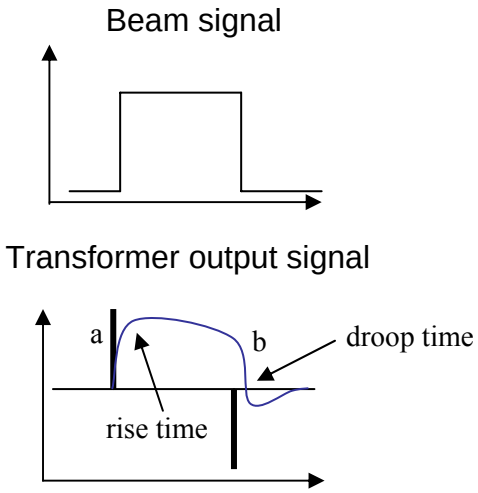

Fig. 8: The ideal output signal from an AC current transformer: (a) infinite output impedance; (b) finite output impedance with stray capacitance and inductance

The rise time of the output signal is determined by cable inductance and stray capacitance:

$$\tau_{\mathrm{rise}} = \sqrt{L_{\mathrm{s}}C_{\mathrm{s}}}$$

and the droop time constant by the cable inductance and the output impedance:

$$\tau_{\mathrm{droop}} = \frac{L}{R + R_{\mathrm{L}}}.$$

By using an active transformer in which the output resistor is replaced by an operational amplifier with gain A and a feedback resistor R_{f} the droop time can be extended until up to a second.

$$\left(\tau_{\mathrm{droop}} = \frac{L}{\frac{R_{\mathrm{f}}}{A} + R_{\mathrm{L}}} \approx \frac{L}{R_{\mathrm{L}}}\right).$$

In low-energy machines the beam needs to be re-focused in a tight mesh of focusing magnets leaving little space. This implies that the instruments may be situated close to high powered pulsing equipment which will cause electromagnetic interference. The transformer is therefore enclosed in shielding layers consisting of soft iron and μ-metal layers.

On low-energy machines we often have beam pulses of several hundred microsecond length which can easily be digitized with a fast analog-to-digital converter. The converted signal can then be treated digitally; baseline shifts due to surrounding elements can be determined and corrected for.

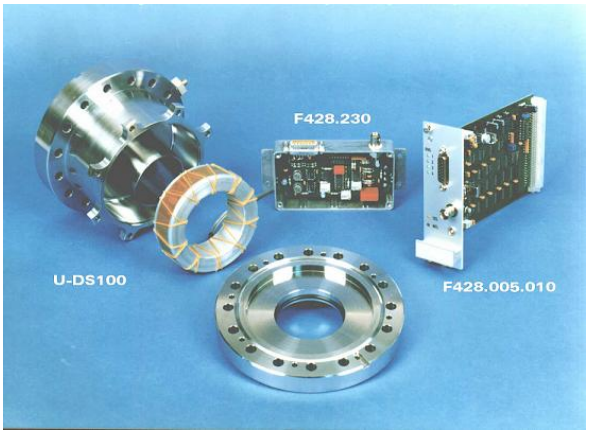

Fig. 9: An AC current transformer and its electronics

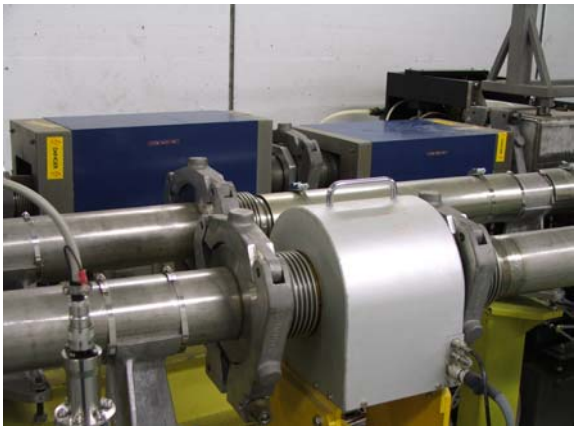

Fig. 10: A current transformer installed in the beam line

The transformer must be calibrated, which is usually done with a high-precision current source. The current signal is injected into the transformer through a separate calibration winding. This may be done only once in a dedicated calibration procedure where the results are stored in tables and re-used by the read-out program. It can, however, also be done for each beam pulse by injecting the signal shortly before or after the arrival of the beam pulse and reading it with the measurement data (see Fig. 11).

Figure 12 shows a typical transformer measurement: the beam intensity (bar graph) is observed along a transport line and losses between two transformers can easily be spotted.

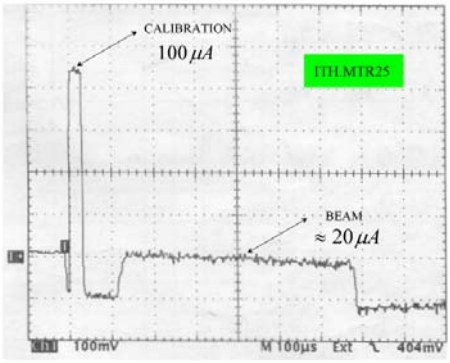

Fig. 11: A beam pulse and its calibration pulse

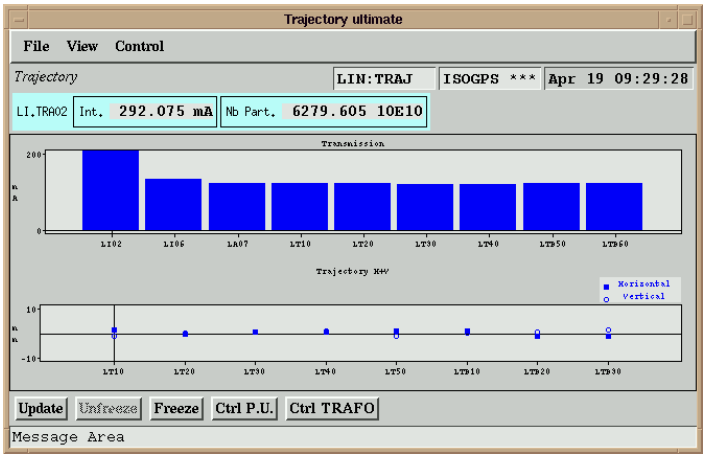

Fig. 12: Loss measurement using AC transformers

2.3 DC current transformers

In order to extend the transformer's bandwidth down to DC, needed, for example, for storage rings, in which the beam may stay for hours, the principle of the zero flux magnometer is applied (Fig. 13). Is uses a magnetic modulator exploiting the non-linear magnetization curve of ferromagnetic material. Two cores are fed in opposite phase with a modulation current driving the cores into saturation. The signals from secondary windings connected in series will produce a zero sum signal. Since the

magnetization curve will be perfectly symmetric, only odd harmonics of the modulation frequency will be present in the modulation spectrum. It is clear that the pair of coils must be carefully matched such that the induced signal after subtraction is minimized.

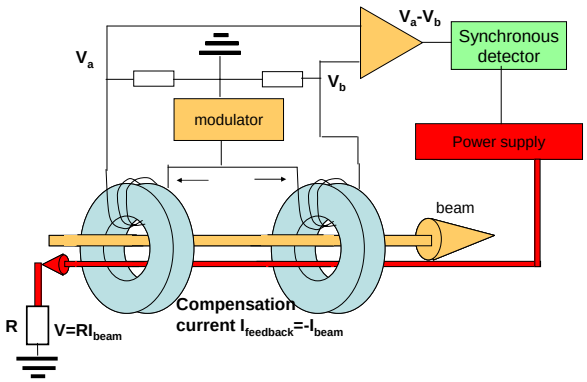

Fig. 13: The zero flux magnetometer

A DC current passing through the coils introduces a bias in the excitation, the sum signal becomes non-zero and even harmonics, in particular the second harmonic, will appear in the spectrum.

A synchronous detector extracts the information about the signal amplitude and phase of the component at the second harmonic of the modulation frequency. This signal is used to create a feedback current cancelling the flux induced by the beam. This feedback current is finally measured.

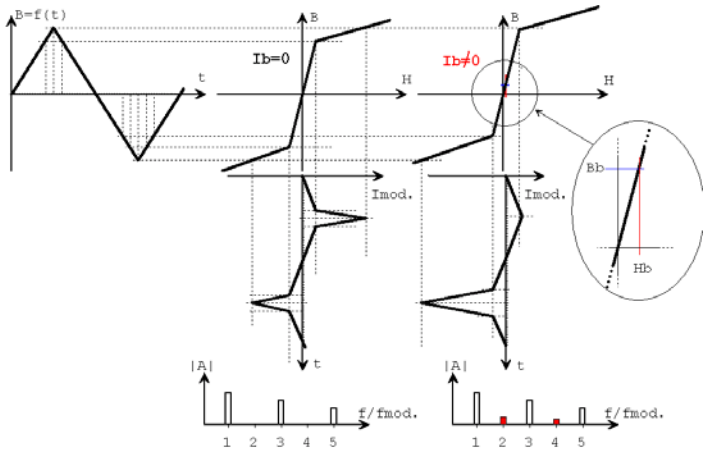

Fig. 14: Modulation of a DCCT left: without beam, right: with beam

When measuring beam intensity in low-energy synchrotrons, it is actually not the DC current but the number of particles or number of charges which is the parameter of interest. Since the revolution frequency changes due to the increasing speed of the particles, the current will also increase. One can extract the number of charges by calculating the particle speed from the measured magnetic field of the synchrotron's bending magnets and applying β-normalization.

3 Profile and emittance measurements

3.1 Interaction of a particle beam with matter

Most of the profile measurement devices rely on an intercepting sensor to generate a signal containing the information of beam density at a certain position or angle. The signal may be the emission of light or it may be a current created through the ionization of a gas or through secondary emission of

electrons from the material's surface. In order to estimate the signal power, we must look into the mechanism of energy transfer from the accelerated particle to the intercepting matter.

All the effects result from Coulomb interaction of the incoming beam particles with the sensor matter.

When a beam particle at high speed passes near an atomic shell electron of the intercepting material, the force F_s along the particle's path cancels, while the transverse force does not (Fig. 15). This means that ejected electrons will be observed at right angles with respect to the beam particles' movement. Head-on collisions (with very small impact parameter b, where electrons have high energies (delta electrons)) are very rare and the electron energy is generally below 20 eV.

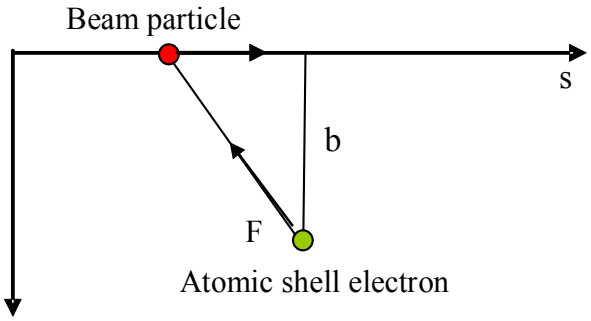

Fig. 15: Beam particle interacting with an atomic shell

The energy loss of an ionizing particle in matter is described by the Bethe–Bloch formula (Fig. 16):

$$-\frac{\mathrm{d}E}{\mathrm{d}x} = 4\pi N_\mathrm{A} r_\mathrm{e}^2 m_\mathrm{e} c^2 \frac{Z_\mathrm{T}}{A_\mathrm{T}} \rho \frac{Z_\mathrm{p}^2}{\beta^2}\left[\ln\frac{2m_\mathrm{e}c^2\gamma^2\beta^2}{I} - \beta^2\right]$$

with the following constants:

- N_A: Avogadro's number
- m_e and r_e: electron rest mass and classical electron radius
- c: speed of light;

the following target material properties:

- ρ: material density
- A_T and Z_T: the atomic mass and nuclear charge;

and the particle properties:

- Z_p: particle charge
- β: the particle's velocity and

$$\frac{1}{\gamma = \sqrt{1-\beta^2}}.$$

Two facts are interesting to note: the quadratic dependence on the particle charge, meaning that the energy deposition of high-charge-state heavy ions is much higher than for singly charged protons, for example, and the fact that low-energy particles deposit much more energy in the target material than higher energy ones. At ~1 GeV a projectile particle is called minimum ionizing because its energy transfer is at a minimum.

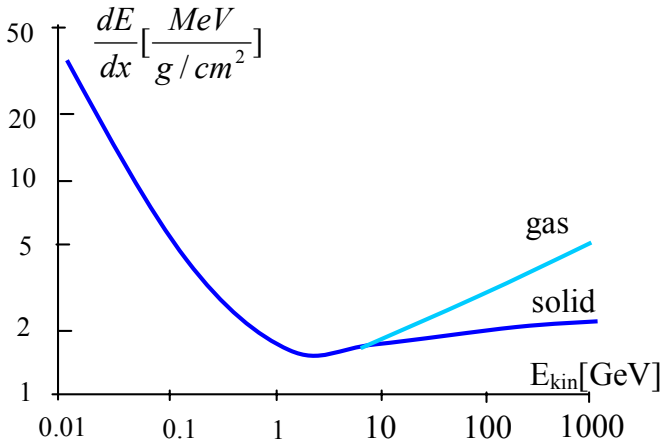

Fig. 16: The Bethe–Bloch formula

3.2 Scintillating screens

Scintillating screens were used in cosmic-ray experiments even before the invention of particle accelerators and have been in common use ever since. It is their simplicity, low cost, and power of conviction, which makes them so attractive. A measurement can hardly be more intuitive than to see a beam spot right in the centre of a scintillation screen. In its simplest form (Fig. 17), a plate of scintillating material with a graticule printed on it is inserted into the beam under an angle of 45º. Through a viewport, located at 90º with respect to the beam, a camera observes the screen. Often a second viewport is used to illuminate the screen so that the graticule can be seen.

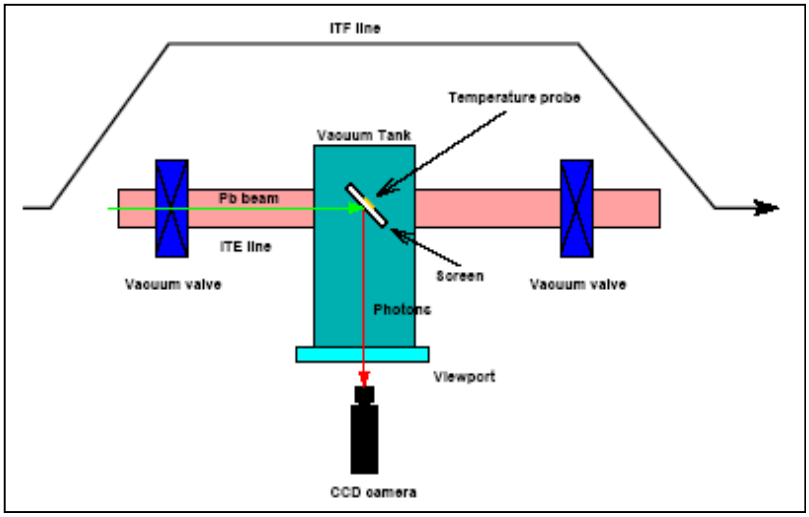

Fig. 17: Scintillating screen assembly

At low energies and low intensities, the radioactivity induced in the accelerator environment is low enough to use cheap commercial CCD cameras. At higher intensities, however, the CCD chip will quickly be destroyed through radiation. In this case Nuvistor-based cameras are used. Also, cheap lenses turn brown under radiation and must be replaced regularly. The same is true for the viewports.

As we have already seen during the discussion of Faraday cups, the deposition of energy and charge in the intercepting material may lead to heating problems and electrical charging and may even destroy the detector.

Table 2: Scintillating material properties

Material	ρ g/cm^3	C_p **at 20°C** J/gK	k **at 100°C** W/mK	T_{max} °C	R **at 400 °C** Ω.cm
Al_2O_3	3.9	0.9	30	1600	10^{12}
ZrO_2	6	0.4	2	1200	10^3
BN	2	1.6	35	2400	10^{14}

To ensure that the screen used at CERN's ion facility will survive bombardment with lead ions, several scintillating materials have been tested in the beam. The scintillating material was exposed to 4 MeV/u lead ion pulses of 50 µA and 200 µs at a pulse rate of 5 Hz. While Al_2O_3 (chromox) screens showed an important decrease in their scintillating efficiency, ZrO_2 screens turned out to be more stable (see Fig. 18). Chromox screens are largely used in higher energy proton machines and were used as reference. Even though the screen had been clearly affected by the impinging beam (Fig. 19), its scintillation properties remain unchanged.

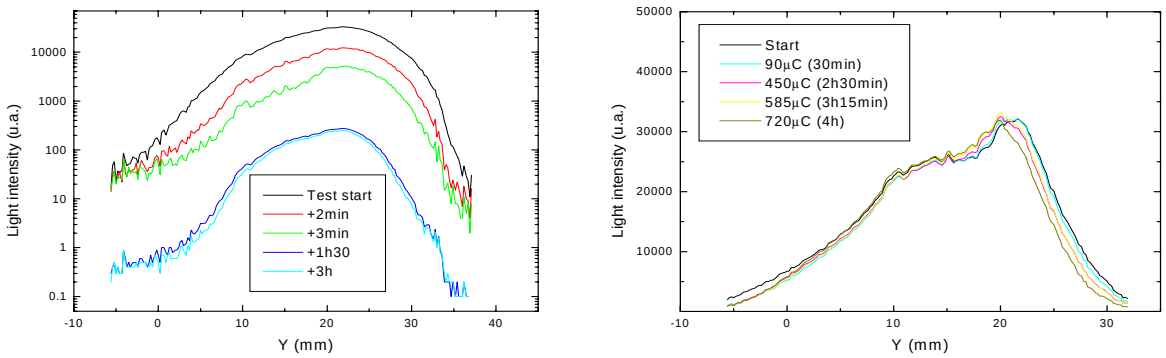

Fig. 18: Light emission efficiency after bombardment with ions (left: Al_2O_3, right: ZrO_2)

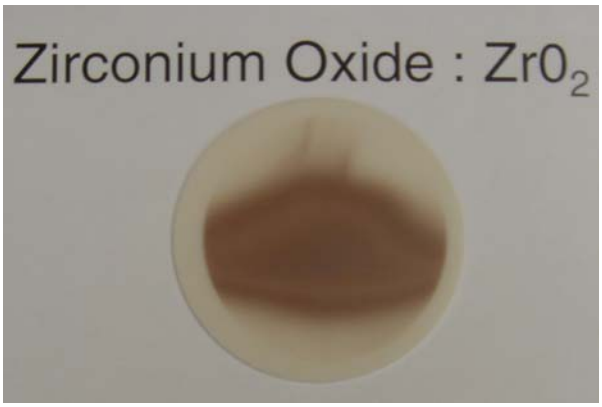

Fig 19: Alteration of the screen of exposure to ion beams

In order to get a more qualitative picture than the furtive glimpse onto a quickly disappearing beam spot, the video signal from the camera can be digitized with a *frame grabber,* keeping the digitized image in a frame memory. This converted image may then be used to either re-create a video signal, allowing observation until the next beam pulse passes, or it may be read out by a computer for further data treatment as has been done for Fig. 18.

3.3 In/out mechanisms

Sensors being inserted into or traversing the beams often require complex mechanical assemblies. The sensor position must be precisely known and often the device must be inserted and extracted in a very short time (some 200 ms). This leads to a multitude of different assemblies, driven by an electric motor (DC motors, AC motors or stepping motors are all in use) or by pneumatic systems. Both linear and rotating systems are exploited. Figures 20 and 21 give a few examples.

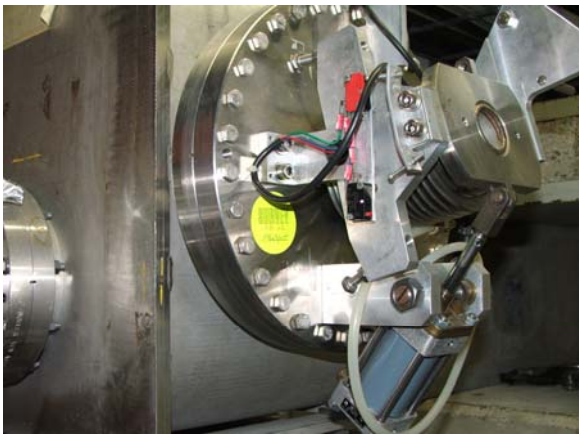

Fig. 20: A pneumatic in/out mechanism

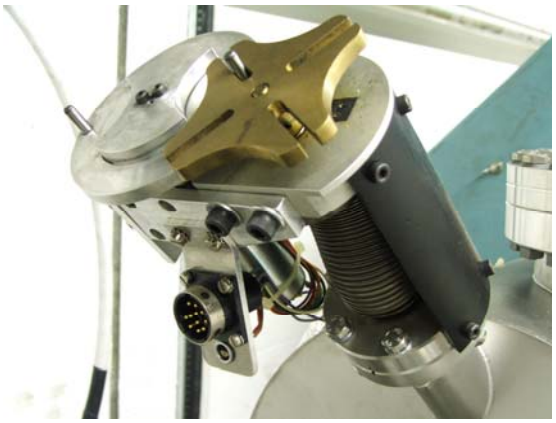

Fig. 21: A rotary mechanism for four screens

The mechanism on the secondary emission grid (Fig. 22) allows inserting the device as well as rotating it.

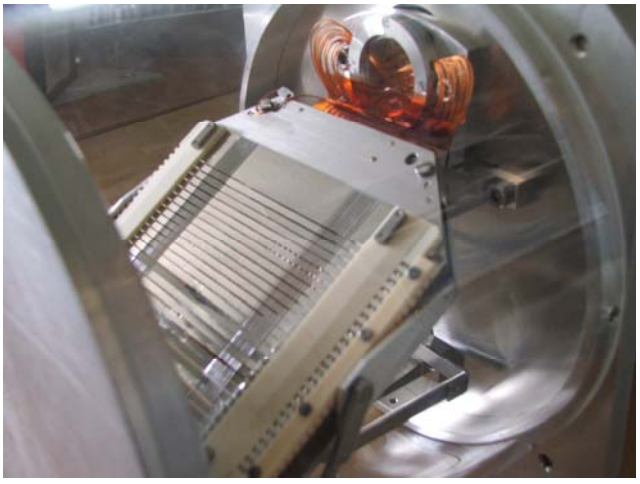

Fig. 22: Secondary emission grids

3.4 Secondary emission detectors

In order to measure the transverse distribution of the particle beam, a wire array or a set of very thin metal ribbons is inserted into the beam. By interacting with the wire material, secondary electrons are emitted and a voltage potential is created. This results in a current flowing back onto the wire which is amplified and measured. The ejected electrons are collected through clearing fields, created by a polarization voltage of some 100 V, avoiding the build-up of an electron cloud on the surface of the ribbons. Figure 22 shows a secondary emission grid with its mechanical assembly. Since each wire or ribbon delivers a signal proportional to the number of particles hitting its surface, a beam profile, the projection of the particle density distribution, can be determined.

3.5 Wire scanners

When trying to measure beam profiles in circular machines, the secondary emission grid cannot be used. Firstly, the beam blow-up caused by the scattering of the beam particles in the wire material will falsify the measurement and secondly, multiple passages of beam particles will deposit thermal energy, which will cause the destruction of the SEM grid wires for any beam of reasonable intensity.

(SEM grids have been used in circular machines for the measurement of emittance matching, measuring profiles on multiple turns but only some 20 consecutive profiles were taken into account, limiting the blow-up effect and dumping the beam after these 20 turns in order to spare the detector.)

A wire scanner (Fig. 23) consists of a thin straight wire of light material, often SiC or carbon which is passed through the beam. This limits the energy deposition in the wire [Bethe–Bloch: $\mathrm{d}E/\mathrm{d}x \propto \rho(Z/A)$]. If the beam energy is high enough, a secondary particle shower is created which is detected by a scintillator–photomultiplier assembly outside of the vacuum chamber (Fig. 24).

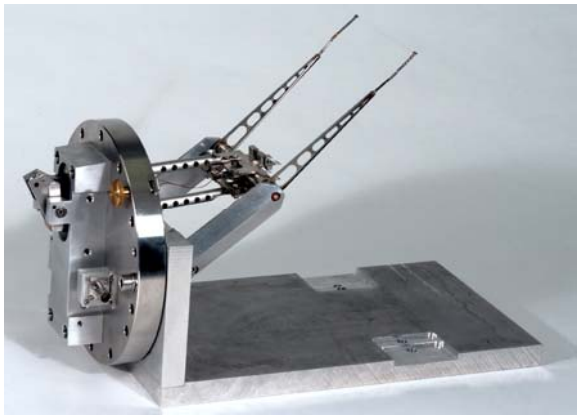

Fig. 23: A fast wire scanner

Fig. 24: Fast wire scanner with scintillator and photomultiplier

The wire speed must be as high as possible in order to limit beam blow-up and to avoid measurement errors due to adiabatic damping (see Section 3.6) and current increase due to change of the revolution frequency when measuring during acceleration. Currently speeds of up to 20 m/s have been achieved.

At beam energies below 150 MeV, the minimum energy needed to create pions, hardly any secondary particles are seen on the scintillator (Fig. 25).

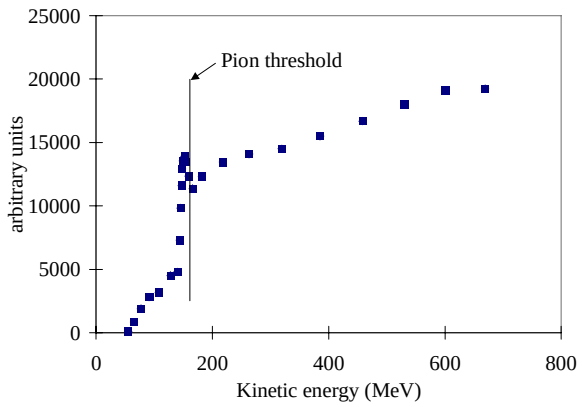

Fig. 25: Pion threshold for the production of secondary particle showers

If, however, the wire is mounted electrically isolated, the secondary emission current from the wire can be measured. In this case, the low energy of the primary beam particles is not an issue. As Fig. 26 demonstrates, very clean profiles can be measured with secondary emission, while the photomultiplier signal becomes very noisy and asymmetric due to geometrical effects depending on the placement of the scintillator.

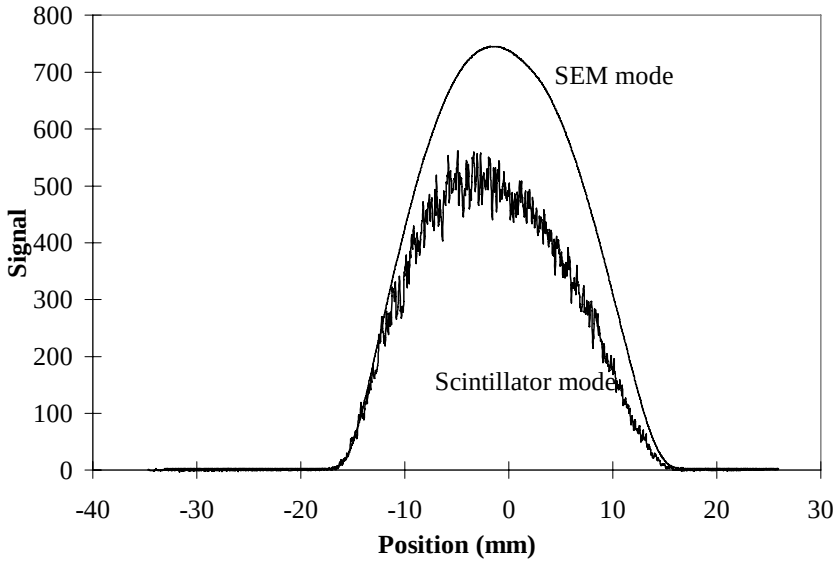

Fig. 26: Profiles at low beam energy

Profiles of partially stripped ions cannot be measured with such a wire scanner because the interaction of the ion with the wire will induce stripping (one or more electrons will be removed from the ion's atomic shell) and the ion will be lost.

One can, however, use the stripping effect to measure the betatron amplitude distribution. In this case the wire scanner (or a scraper) is used to scrape off the beam starting from the outside of the particle distribution and finishing as soon as the core of the beam has been reached. The losses are observed on a DC current transformer. Figure 27 shows a typical loss curve from which the amplitude distribution and the intensity profile can be determined.

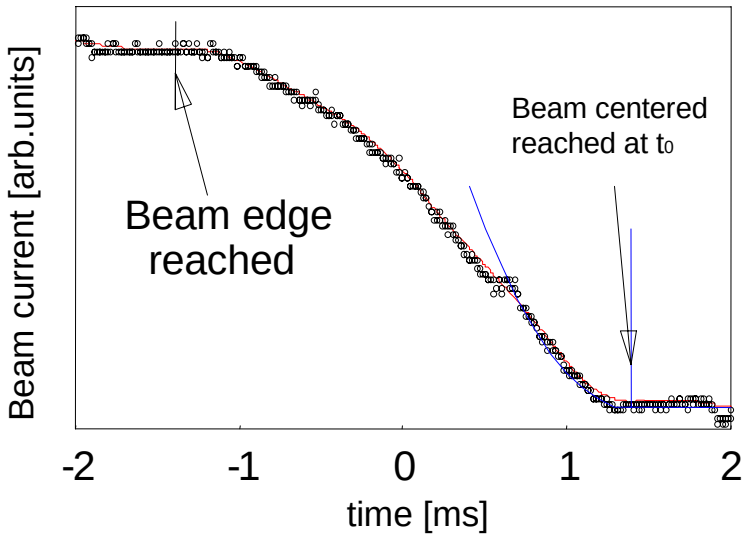

Fig. 27: Betatron amplitude distribution

3.6 Emittance measurements

Particles in a beam have a velocity vector which points mainly into the direction corresponding to their nominal orbit. There are, however, small deviations in transverse direction, which are corrected by the accelerator's quadrupoles.

$$\vec{v}_{\text{particle}} = v_s \hat{u}_s + v_x \hat{u}_x + v_y \hat{u}_y$$

The particles therefore oscillate transversely around their nominal trajectory. If we plot the positions (x) of all particles on one axis and their transverse angle (x') on the other, we get a two-dimensional phase space distribution.

The surface in which a certain percentage of all particles will be found forms an ellipse whose area is called the transverse emittance ε. As the particles move along an accelerator ring or a transfer line, the ellipse changes its shape but the surface stays the same (at least as long as the particle is not accelerated).

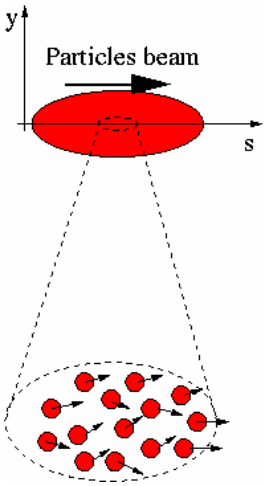

Fig. 28: The beam's transverse velocities

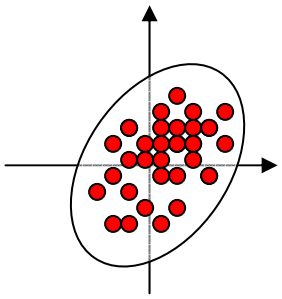

Fig. 29: Phase space plot

Imagine a particle having a certain offset from the nominal orbit and a certain angle with respect to the nominal direction s. This corresponds to a point in phase space (see Fig. 30). If this particle moves through a drift space, its angle will not change, however, its offset position from the nominal orbit will increase, which results in a move in the horizontal direction in phase space. If the particle sees an (infinitesimally small) quadrupole it will not change its position, however, its angle will be modified resulting in a horizontal movement in phase space.

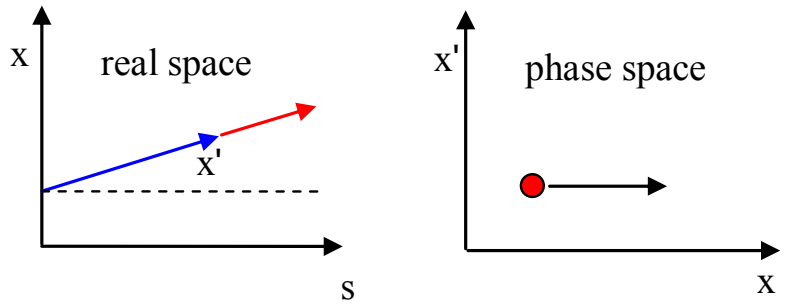

Fig. 30: Movement of a particle in a drift space

If a slit is placed in the beam, it cuts out a slice of particles all having the same position with respect to the nominal orbit. If these particles pass through a drift space, big angles will result in a large displacement, while small angles will provoke only a small position offset. Angles are therefore converted into positions and can be measured with a profile measuring device like a SEM grid or a scintillating screen.

When the slit is moved across the beam and the angle distribution is measured for each position, the phase space can be *scanned* and the phase space distribution can be measured (Figs. 31 and 32).

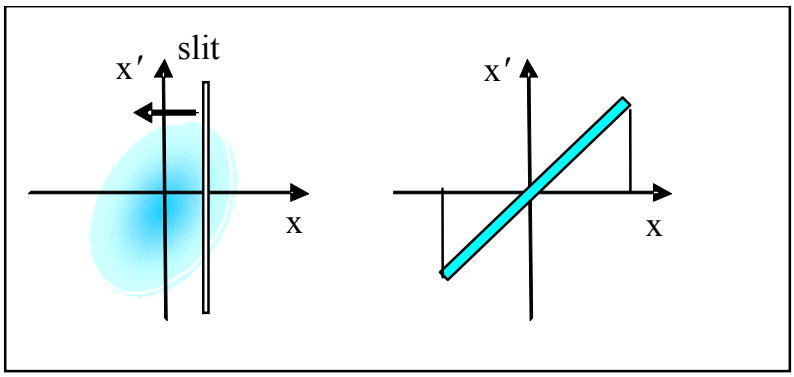

Fig. 31: Phase space scan

The position resolution is determined by the slit size and the number of steps at which the angle distributions are measured. The angular resolution depends on the profile detector (the distance between the wires in the case of a SEM grid) and on the distance of the slit to the profile detector.

The disadvantage of this method is also rather obvious: When a high position resolution is required and the machine duty cycle is low, the measurement can easily take several minutes and fluctuations form one beam shot to the next will result in measurement errors.

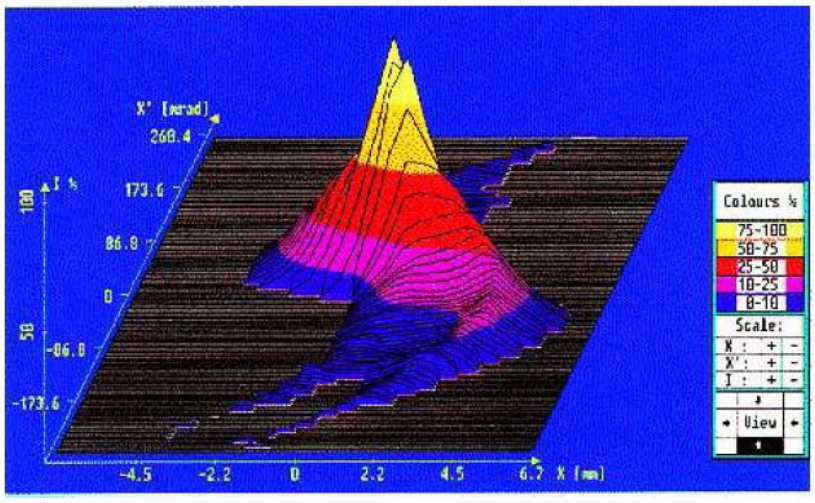

Fig. 32: Results from a phase space scan

These problems can be solved by sweeping the beam in front of the slit using a pair of kicker magnets powered in opposite phase (Fig. 35). Of course a dedicated beam line is needed in this case, representing a non-negligible investment. Now the angle distributions must be sampled at high frequency as the beam is swept. Like this an emittance scan can be made even within a single pulse of some tens of microseconds length.

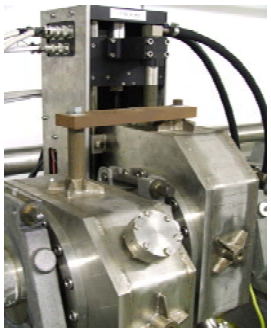

Fig. 33: Slit

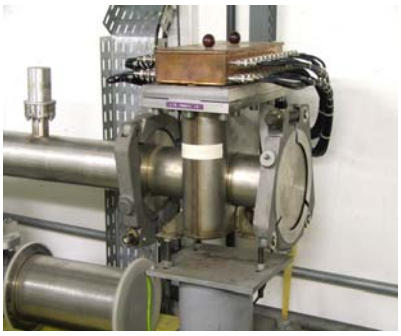

Fig. 34: SEM grid

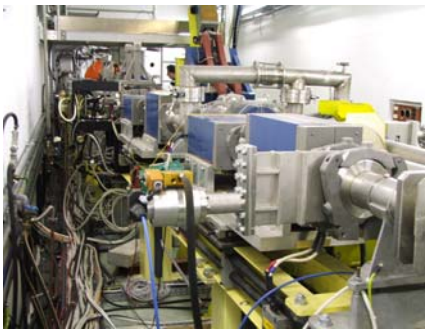

Fig. 35: Horizontal and vertical kicker magnets

Figure 36 shows the result from a single-shot phase-space scan. As can be seen, not only the emittance (area of the ellipse) but also its geometrical parameters (Twiss parameters), important for matching of the transfer line to the receiving machine, can be determined.

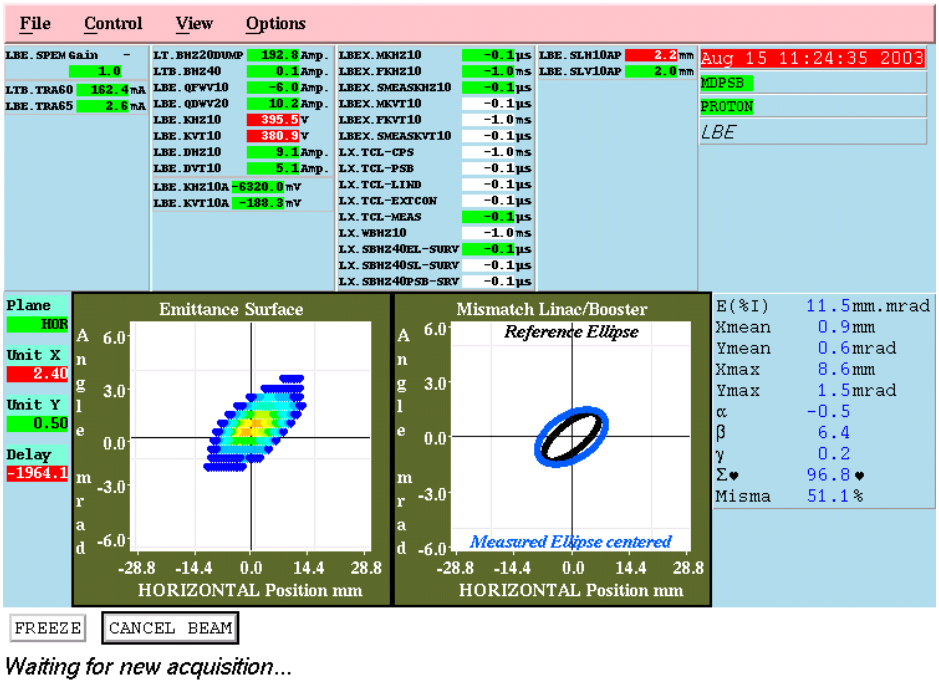

Fig. 36: Result of a single-shot phase-space scan

Another, less costly possibility to measure the transverse emittance on a single beam pulse is to use a plate with a series of slits. The position resolution is then given by the slit distance and one must make sure that the angle distributions measured on the profile detector (in this case usually a scintillator screen) do not overlap. On low-energy beams, where the beam spots are usually rather large, this may be possible. The method is not exactly new and I learned from a former colleague that he had participated in measurements of this kind on the CERN proton Linac in the early 1970s, where a photographic plate was used as 'profile detector'. The plate was inserted into the measurement line, a few beam shots where used for exposure, and the photograph of the slit images was developed. The evaluation of the angular distributions was done with a ruler and *a trained eye*. Even if the principle of the measurement is still the same, electronic means like image digitization associated with computer data treatment have made this type of measurement a routine operation, whereas before it was only possible during dedicated machine development sessions.

If instead of using multiple slits one uses little holes, then the emittance in horizontal and vertical phase space can be measured at the same time. The method is called the *pepperpot* method because the plate containing the holes resembles a pepperpot (Fig. 37).

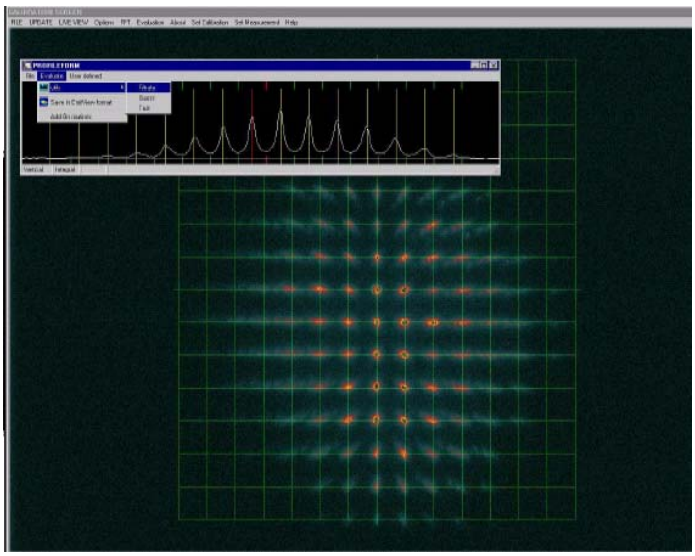

Fig. 37: A pepperpot measurement

When a beam is accelerated, its emittance shrinks due to adiabatic damping (Fig. 38). This effect can easily be visualized: the particle's velocity component in the forward direction is increased, which results in smaller transverse displacements at the same longitudinal distance. The normalized emittance $\varepsilon_{\text{norm}} = \varepsilon_{\text{physical}} \beta\gamma$ (with β the particle speed and $\gamma = 1/\sqrt{1-\beta^2}$ the Lorentz factor), however, is constant under ideal acceleration conditions.

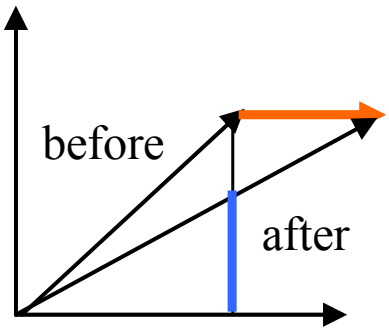

Fig. 38: Adiabatic damping

4 Position measurements

4.1 Beam-position monitors

In order to measure trajectories through a transport line or beam orbits in a circular machine, beam-position monitors (BPMs) are needed. These devices make use of either the beam's electric or magnetic field and exist in a large variety. Since they pick up the beam's fields they are also commonly called *pick-ups*.

An electrostatic pick-up (coupling to the beam's electric field) is shown in Fig. 39. We call it shoe-box pick-up because its form resembles a shoe-box which is diagonally cut into two halves.

If a beam passes with a certain average displacement with respect to its nominal central orbit, it induces a different amount of charge on each of the two halves. Since the box is cut in a linear fashion, the position can easily be calculated:

$$x \propto \frac{U_L - U_R}{U_L + U_R}$$

where $U_L - U_R$ is often called the Δ signal and $U_L + U_R$ the $\sum$ signal. A typical trajectory measurement in a transfer line is shown in the lower part of Fig. 40.

Many ingenious cuts have been invented in order to measure horizontal and vertical positions with a single device.

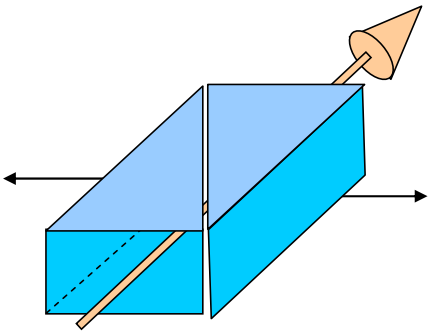

Fig. 39: Shoebox pick-up

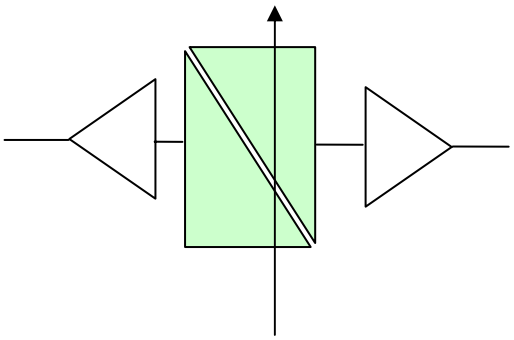

Fig. 40: Inducing charges on an electrostatic pick-up

If instead of a box-type pick-up a cylindrical geometry is chosen, the electrodes have a more complex form,but the Δ signal can still be made linear with the beam displacement. Cutting a cylinder diagonally and then unfolding it results a sine curve. If the negative part of the sine is flipped ($|\sin(x)|$) then a V cut will result and one can create horizontal and vertical electrodes. The pick-up in Fig 41 can measure positions in both planes (there are four electrodes) and is perfectly linear with displacement, as can be seen in the calibration measurement of Fig. 42.

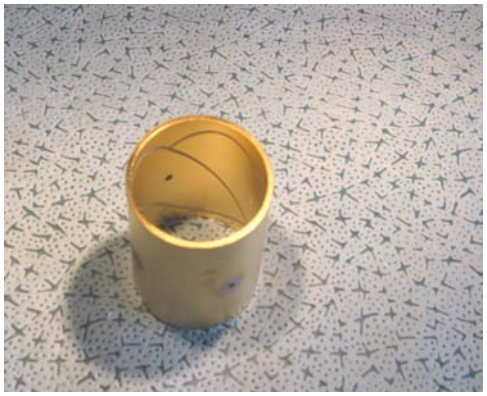

Fig. 41: Cylindrical pick-up

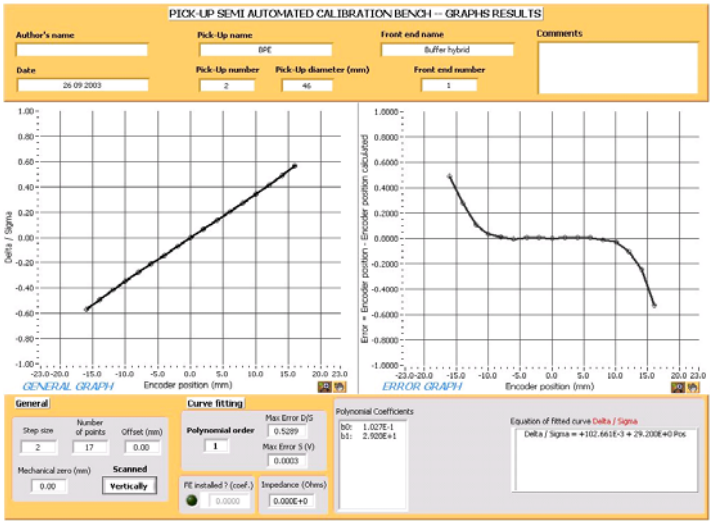

Fig. 42: Calibration measurement of the pick-up

4.2 Tune measurements

It is in circular machines where position measurements are most important. If a beam is injected with a wrong angle or position, it will start to oscillate and the amplitude of these *betatron oscillations* can be used to determine the error made and to correct for it. On the other hand, the oscillation may be used to determine the machine *tune* (the number of oscillations per turn), which is one of the most important parameters in a circular accelerator because it determines the stability of the beam in the machine. In Fig. 43 the lower part shows injection oscillations and the upper part the Fourier transform of the signal with a peak at the non-integral part of the tune. If many pick-ups are installed all around the ring, then the full oscillation can be followed. It is, however, also possible to determine the tune with a single pick-up and a kicker inducing betatron oscillations deliberately. The beam is then observed during each consecutive passage through the same pick-up.

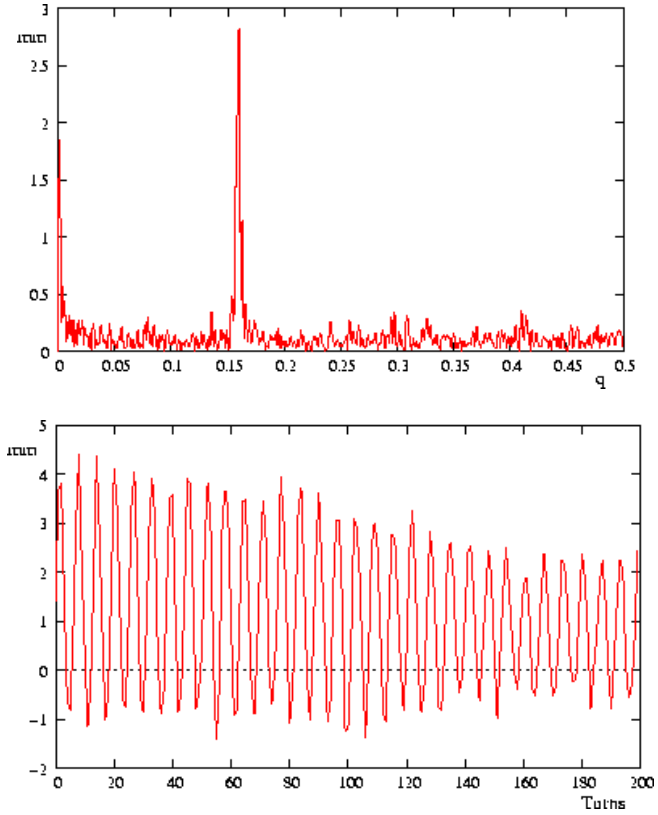

Fig. 43: Tune measurement

4.3 Closed-orbit measurements

When using several pick-ups around the ring and averaging their readings at each passage of the beam, the closed orbit of the machine can be measured. This orbit takes into account all deficiencies of the machine like misalignment, field errors, and the like and the measured orbit may differ from the ideal beam path determined by the centre of the quadrupoles. The position readings may be used as input for a feedback loop to actively correct the beam orbit.

Position measurements in a low-energy synchrotron can be a tricky business especially if several bunches are present in the machine. Bunches may even have largely different properties like different intensities. Figure 44 shows signals from orbit pick-ups during a double batch injection. First a batch of four bunches was injected which can be seen in the first two revolutions and then another two bunches are added. The big signal corresponds to the sum signal while the small one is the delta signal. A rather large excursion for the two newly injected bunches can clearly be seen. Since in small

hadron synchrotrons the particles are largely non-relativistic, their speed increases during acceleration, which means that their revolution frequency also increases. If trajectories or orbits must be measured on a bunch-by-bunch basis, then the system must be capable of tracking the bunches as they circulate in the machine. This may be further complicated by RF gymnastics by which batches of several bunches are compressed into a smaller space in the machine or by bunch splitting (see Fig. 45) or recombination, which even changes the number of bunches in the machine. Very sophisticated digital signal treatment may be needed to solve such problems. In order to become usable in routine operation, such signal treatment should be done in real-time, which means at typical signal bandwidth of some 30 MHz.

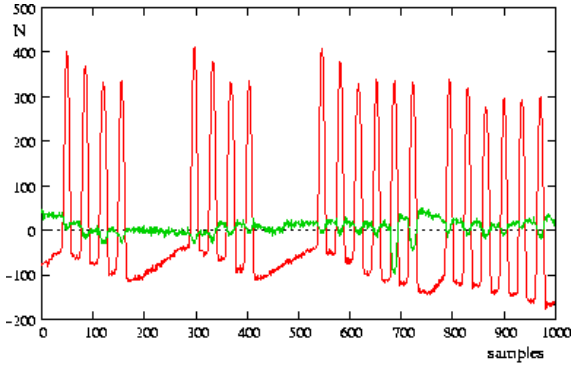

Fig. 44: Double batch injection

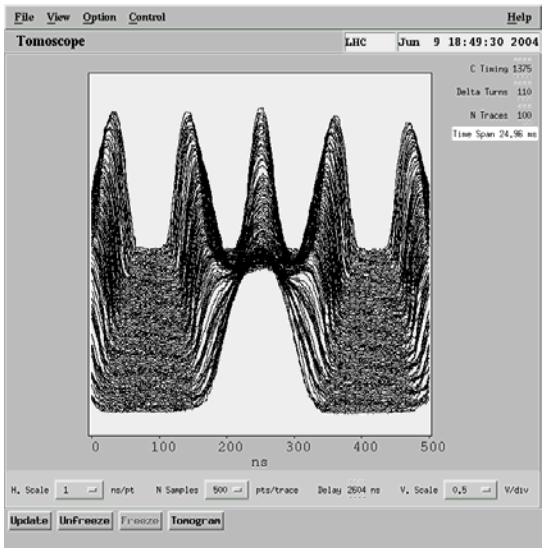

Fig. 45: Triple bunch splitting

5 Further reading

The Joint Universities Accelerator School (JUAS) is an accelerator physics course which is held every year for four weeks in Archamps, France. It extends the university physics curriculum with an academic course that would be difficult to organize at European Universities and is open to students from all European countries. It teaches all fields of machine physics and accelerator technologies, and beam diagnostics is one of the topics. P. Forck from Gesellschaft für Schwerionenforschung (GSI) Darmstadt, Germany, has taught this subject for several years and he has written excellent course notes, which are available at http://www-bd.gsi.de/conf/juas/juas.html together with the course transparencies.

Earlier CAS schools contain articles on beam diagnostics. The one of Jyväskylä contains a course on beam instrumentation written by H. Koziol.

In 1998 there was a CAS school dedicated to Beam Measurement and its proceedings provide more elaborate explanations on how machine parameters may be measured.

For detailed descriptions of measurement techniques or instruments, the proceedings of the bi-annual beam diagnostics conferences DIPAC (Diagnostics and Instrumentation for Particle Accelerators in Europe) and BIW (Beam Instrumentation Workshop in the USA) are interesting sources of information.

6 Conclusion

In two hours of lectures it is possible to give only a crude overview of the field of beam diagnostics. There is a multitude of different measuring principles and instruments and I tried to touch at least on a few of them, emphasizing peculiarities of low-energy machines, like big beam sizes, long pulses etc. I hope that these lectures have convinced you that beam diagnostics is a fascinating field of accelerator technology and that they made you want to further explore this scientific field.

Acknowledgements

I would like to thank E. Bravin, T. Lefevre, V. Prieto, J. Belleman, M. Gasior, L. Søby, P. Odier, C. Bal, P. Forck for interesting discussions, and for help by providing their tables, figures or photographs, or proofreading. Further thanks go to my group leader H. Schmickler, who allowed me to put the necessary effort into the preparation of these lectures and to my wife who saw me typing away on my computer for many long evenings.